Journal of Rehabilitation in Civil Engineering 11-4 (2023) 91-121

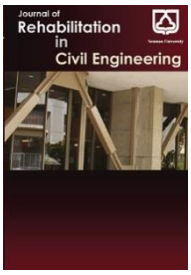

journal homepage: https://civiljournal.semnan.ac.ir/

Experimental and Analytical Study on the Longitudinal Shear Bond Behaviour of Basalt Textile-Reinforced Concrete Composite Slab

Aniket A. Shirgaonkar [1,*]; Yogesh D. Patil [1]

1. Department of Civil Engineering, Sardar Vallabhbhai National Institute of Technology, Surat, India

* Corresponding author: *d17am002@amd.svnit.ac.in*

ARTICLE INFO

Article history:
Received: 11 June 2022
Revised: 20 October 2022
Accepted: 26 March 2023

Keywords:
Composite slab;
Basalt textile-reinforced concrete;
Longitudinal shear bond strength;
Slip.

ABSTRACT

Composite deck slab flooring system is gaining popularity since they allow for simpler, lightweight, and more cost-effective building construction technique. The main constituent materials of a composite slab are profiled deck steel sheet and concrete. Profiled steel sheet serves two purposes: it acts as a main reinforcing structural element as well as a permanent formwork during the construction phase. The efficiency of the composite slab mainly depends upon the shear interaction between concrete and steel decking sheet. This paper contributes to improving the horizontal shear strength of composite slab by utilizing basalt textile reinforced concrete (BTRC) topping. The current research is focused on examining the behavior of this shear bond action and improving its performance even without the shear connectors. Three types of concrete topping and four different shear spans (250 mm, 325 mm, 550 mm, and 625 mm) are the variables of the testing. Based on the load-displacement response, failure mechanisms, maximum strain recorded in concrete/steel, load-slip characteristics, steel-concrete shear bond resistance, and the structural performances of basalt textile-reinforced concrete (BTRC) composite slabs were compared with the conventional concrete (CC) composite slabs. BTRC composite slabs are found to be more ductile than the conventional concrete composite slab, with increased load-bearing and slip resisting capacity. Both the m–k and partial shear connection (PSC) approaches were used to calculate the horizontal shear strength of the composite floor. The m-k technique has proven to be more meticulous than the PSC method.

How to cite this article:
Shirgaonkar, A., & Patil, Y. (2023). Experimental and Analytical Study on the Longitudinal Shear Bond Behaviour of Basalt Textile-Reinforced Concrete Composite Slab. Journal of Rehabilitation in Civil Engineering, 11(4), 91-121. https://doi.org/10.22075/jrce.2023.27455.1664

Nomenclature

N_s	The design value of the plastic resistance of the steel reinforcement to normal force (N/mm^2)
N_{cf}	Compressive force in the concrete
z	Lever arm (mm)
A_p	The effective area of the sheeting corresponding to the slab width (mm^2)
f_y	Yield strength of steel (N/mm^2)
d_p	Distance between the upper fiber and the centroid of the sheeting (mm)
x_{pl}	Height of the compressed concrete block (mm)
b	Width of composite slab specimen (mm)
f_c	Concrete strength under compression (N/mm^2)
L_s	Length of shear span (mm)
L_o	shear span length with overhang (mm)
V_f	Volume fraction (%)
d_p	Effective slab depth to the profile steel sheeting's centre (mm)
V_t	Reaction at the support (N)
σu	Longitudinal shear strength (N/mm^2)
η	Degree of shear connection
N_c	The design value of the normal compressive force in the concrete flange (N)
M_{pr}	Reduced plastic resistance moment of the profiled steel sheeting (N-mm)
M_{pa}	The design value of the plastic resistance moment of the effective cross-section of the profiled steel sheeting (N-mm)
h_t	The overall thickness of the test specimen (mm)
M_{test}	The design value of the plastic resistance moment of the composite section at the test (N-mm)
M_{prd}	The design value of the plastic resistance moment of the composite section with full shear connection (N-mm)

1. Introduction

In steel-framed high rise buildings, profiled decking composite floors have been utilised. Speedy construction work is ensured by the composite floors with profiled decking sheets, which also act as concrete formwork. Cold-formed steel profiled deck sheets act as primary tensile reinforcement after hardening of the concrete topping. Figure 1 depicts the elements of the composite slab. These structures are extremely effective at supporting large loads. Because of its remarkable structural behaviour in terms of strength and ductility, composite steel-concrete structural elements have been widely utilised for building floors for a couple of decades across the globe. The composite action between these structural elements requires effective horizontal shear transmission at the interface between the steel decking sheet and the concrete [1]. End anchoring through deck welded studs, mechanical interlock by indentations or embossments in the decking sheet, frictional interlock are all typical forms of efficient shear connection systems in composite slabs [2]. The relative end slip at the steel-concrete contact surface results in a loss of composite action, which has a major impact on the structural performance of the composite slab [3–6]. Composite slab's most dominant failure mode is concrete-steel detachment caused by longitudinal shear, which occurs before vertical shear or bending failure with significant slippage [7]. Researchers have been studying the behaviour of composite slabs for decades by performing full-scale 4-point bending experiments on simply supported and continuous support conditions [7–11]. Some research has focused on the ductile performance and failure mechanism of simply supported composite slabs. The

Eurocode 4 specifies requirements for steel and concrete composite structures [12]. Furthermore, the code's provisions emphasise the design of a typical connection between a composite deck and structural steel, with minimal information on the techniques that strengthen the steel deck's bond with concrete. However, there are numerous articles in the literature that discuss the new schemes that improve the shear bond between the concrete topping and profiled steel deck [13–15]. Daniels et al. (1990) [16] proposed a "New Simplified Method" for predicting composite slab performance. To get the moment-curvature correlation of a composite slab, this unique technique involves data from conventional materials testing and small-scale experimentations with a simple mathematical model. Fallah et al., 2019 [17] examined the application of High-Performance Fiber Reinforced Cement composites for strengthening two-way reinforced concrete slabs. The height of embossments has a significant impact on the shear bond characteristics of composite slabs [18]. The ultimate load capacity is not influenced by variations in concrete compressive strength [19]. Porter and Greimann (1984) [9] used a linear regression correlation between bond strength and reinforcement ratio to get the gradient and intercept coefficients for design. The shear span influences the performance of the embossed profiled composite slab with a normal concrete topping [4,6]. For shorter lengths of shear span, shear bond failure governs the slab's strength, whereas, for longer lengths of shear span, flexural failure governs the strength parameters [4]. The chemical adhesion in the connection between the profiled steel sheet and the concrete is not taken into consideration in EC-4, Lopes and Simoes (2008) [20] established a methodology focused on small scale elemental tests, and it was based on evaluating the moment-curvature.

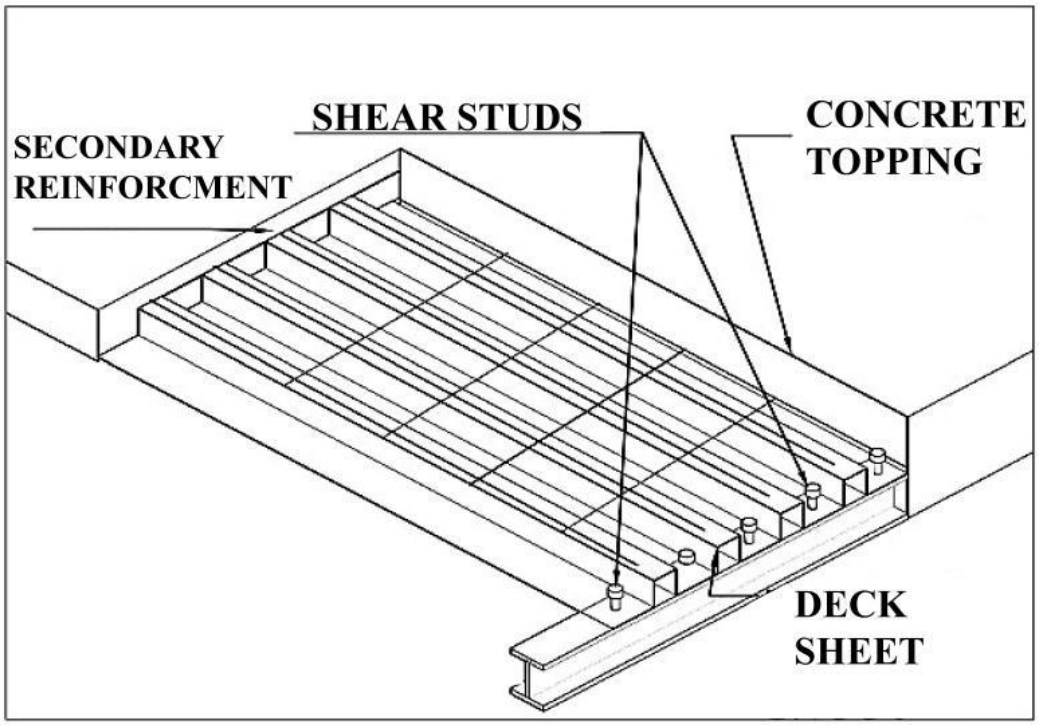

Fig. 1. Details of composite slab.

Textile reinforced concrete (TRC), a novel composite compound made up of fine-grained concrete. Textiles are made up of many different types of fibers and have excellent ductility, impact and corrosion resistance [21]. The textile reinforcement is oriented in the plane of tension, resulting in optimum utilisation of the tensile strength of a fiber [22]. Since the fibers have a small diameter, thinner structural concrete members can be constructed. Carbon, aramid, and alkali-resistant glass fiber-based polymers are the most widely utilised alternative reinforcements in the construction industry [23]. These materials, however, have their own set of benefits and drawbacks. CFRP is a high-strength material that is also costly, whereas GFRP and aramid FRP is less costly but vulnerable to heavy stress and chemical exposures [24]. The basalt fiber reinforced polymer (BFRP) composite is effective in overcoming these significant setbacks. Basalt fibers are made from molten basalt rocks (at 1400°C) [25]. Basalt fiber is a natural fiber that has inherent compatibility with concrete and has resistant to heat and alkalis. Basalt fiber is structurally inert, corrosion-resistant, and has negligible thermal conductance, making it distinctive from any other fiber reinforcement [26]. The strength parameters of basalt fiber reinforced concrete have been investigated by numerous researchers. Basalt fibers have an intrinsic chemical potential to react with cementitious material and also forms calcium silicate hydrate gel, leading to increased strength characteristics of the concrete [27]. The utilisation of basalt fibers to cement mortar reduces substantial dry shrinkage, especially during the early phase [28]. Cement composite materials with basalt fiber have enhanced flexural strength, toughness, and fracture energy. Basalt fiber also has a notably higher elastic modulus (93–115 GPa) than other conventionally used fibers (polypropylene fiber, steel fiber, and polyvinyl alcohol fiber) [29]. Enhanced structural performance and high durability are ensured by BTRC, and it is a feasible alternative among many other FRP strengthening techniques [26]. The reinforcing ratio (layers of BT) has a significant impact on the flexural strength of BTRC [30]. The performance of BTRC is substantially influenced by the reinforcement ratio under tensile stress [31]. The mechanical properties of the concrete are improved by basalt textile reinforcement, while the initial crack stress and strain of the cement matrix are minimized [32]. The tensile properties, compressive/tensile strains, and overall energy absorption capacity of the BTRCs were enhanced by basalt textile reinforcement, although early crack characteristics of the concrete mixture were lowered [31]. The majority of studies have focused on the performance of CC composite slabs. Recent research, on the other hand, has shown a strong interest in exploring the mechanical characteristics and failure mechanism of composite floors composed of lightweight concrete [33]. Light weight concrete (LWC) composite slab improved the structural performance due to enhanced ductility and energy absorbing capacity of LWC. However, in terms of strength and shear bond resistance, Engineered Cementitious Composite (ECC) composite slabs showed better structural behaviour than Self-compacting concrete (SCC) composite slabs [34]. Composite slabs with lightweight woodchip concrete (LWC) also achieved higher shear bond strength and ductility than the CC composite slab [33]. The majority of prior studies has centred on composite floors with normal concrete and

lightweight concrete toppings. Perhaps the performance of textile reinforced concrete composite slabs has received that much attention.

1.1. Research Significance

The potential benefit of basalt textile mesh to be utilised in composite floor slabs is investigated in this paper. The analytical and experimental outcomes give a better insight into the longitudinal shear bond behaviour of BTRC composite slabs. Composite floors with typical concrete toppings have drawbacks such as a brittle failure mechanism and a reduced ductility value [35]. The proposed BTRC-based composite slab can overcome these drawbacks by enhancing composite action and stiffness while also strengthening the shear bond. The failure mechanism of a composite slab with BTRC is investigated in the present study. The structural behaviour of BTRC composite slabs and CC composite slabs were evaluated by experimental and theoretical analyses of load-displacement response, failure modes, strain reported in concrete/steel surfaces, load-slip results, and steel-concrete bond strength. A four-point flexural testing method was used to investigate the composite behaviour, which was performed as per Eurocode-4 specifications.

2. Materials

2.1. Profiled deck sheet

Zinc-coated (275 gsm) profiled deck steel sheets with a thickness of 1 mm were utilised to fabricate all ten composite slab specimens. In this investigation, the length, width, and thickness of the profiled deck sheet were 2750 mm, 605 mm, and 50 mm, respectively. The geometry profile decking sheet used in the present study is illustrated in Figure 2. Table 1 summarises the mechanical and geometrical characteristics of the steel decking sheet. The sheets are embossed with chevron-shaped patterns. Before casting, the profiled deck sheets were cleaned. In order to decrease the preliminary stresses and strains in the slabs, sheets were entirely supported on the level floor throughout the casting.

Table 1. Properties of profiled deck steel sheet

Property	Value
Sheet Thickness (t)	1 mm
Unit weight	5.84 kg/m
Tensile Yield strength f_{yp}	340 MPa
Cross-section area A_S	745 mm^2
Width	635 mm
Length L	2700 mm
Slab depth h_t	120 mm
Height of neutral axis e	24.79 mm
Hogging moment capacity M_{pa}	5.8 MPa

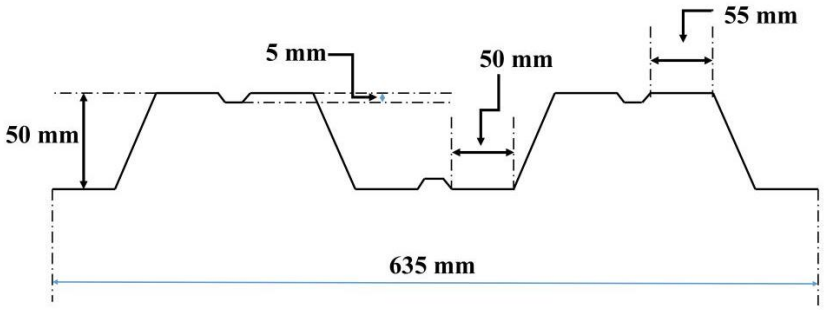

Fig. 2. Geometrical details of the profiled decking sheet (mm).

2.2. Concrete

Table 2 presents the mix of concrete. The concrete mix was made with ordinary Portland cement (53 grade) with a specific gravity of 3.11 [36]. As a fine aggregate, river sand that met the IS 10262 Zone-II requirements was utilised [37]. The specific gravity of the fibers was reported at 2.63. Table 3 summarises the concrete testing results as an average. To investigate the strength parameters of CC, compression tests, flexural tests, and split tensile tests were performed [38,39].

Table 2. Mix design for concrete (per m^3).

20mm aggregate + 10 mm aggregate (Kg/m^3)	Sand (Kg/m^3)	Cement (Kg/m^3)	W/C ratio
1123	828	420	0.45

Table 3. Mechanical properties of concrete.

	Compressive Strength (MPa) (28 days)	Flexural Strength (MPa) (28 days)	Splitting Tensile Strength (MPa) (28 days)
Sample 1	35.06	4.35	3.67
Sample 2	33.8	4.68	3.82
Sample 3	37.1	4.28	3.96
AVG.	**35.32**	**4.54**	**3.62**

2.3. Basalt textile

The maximum size of aggregate used in concrete is 20 mm so the basalt textile mesh utilised in composite slabs was 25mm x 25mm, as it can act compositely with the concrete. The chemical composition of the basalt textile provided by manufacturers are depicted in Figure 2, respectively. The chemical composition of basalt fiber is shown in Figure 3. The main component is silicon dioxide (57%) which provides fiber its strength characteristics. The basalt textile contained 100 filaments, each with a diameter of 16 mm. Tensile testing were carried out using the MTS Criterion Series 40 system at a loading rate of 0.5 mm/min in accordance with Chinese Standard (GB/T 3362,2005) [40]. (Test method for tensile properties of carbon fiber multifilament). Table 4 provides a summary of the results of the basalt textile strip.

Table 4. Properties of basalt textile.

Tensile strength (MPa)	Young modulus (MPa)	Elongation at break (%)	Mesh size	Density g/cm^2
1160	67000	1.8	25 mm X 25 mm	2.33

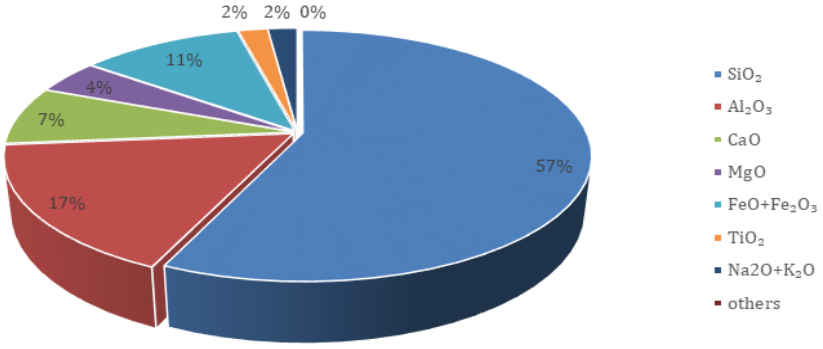

Fig. 3. Chemical composition of basalt fiber.
(Information is provided by Hydro Design Pvt. Ltd, Delhi, India)

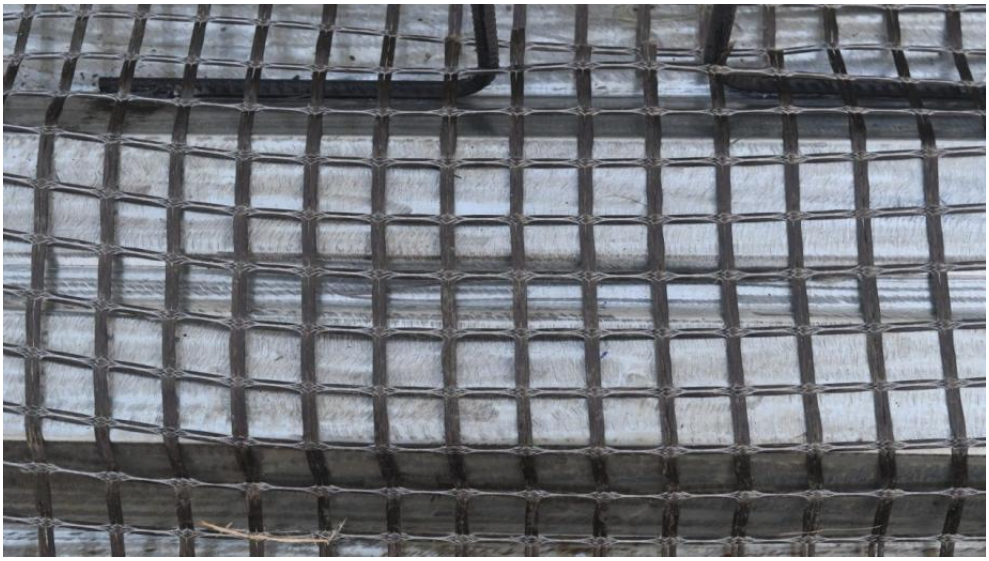

Fig. 4. Basalt textile (25 mm x 25 mm).

3 Experimental programme

3.1. Preparation of test specimen

A new form of a composite slab with CC and basalt textile-reinforced concrete was studied in ten distinct slab configurations. Three types of concrete topping for composite slabs were adopted in the current experimental study: basalt textile at the tension region of the slab (BTRC-T), basalt textile at the tension and compression regions of the slab (BTRC-TC), and CC topping (CC). The specimens with basalt textile (8 specimens) were categorised into four groups of two; two slab specimens were tested for shorter shear span lengths, and the other two specimens were tested for longer shear span lengths.

Shear span is the distance between the points of concentrated applied load and nearby Reaction force. According to EC4, shear spans should be between L/3 and L/5 in length for longer shear spans and between L/7 and L/10 in length for shorter shear spans. Specimen designation is represented in Table 5. Two specimens were cast and tested for shear span lengths 250 mm (L/10) and 625 mm (L/4) for the CC composite slab. Basalt textile (735 mm x 2700 mm) is initially placed over the decking sheet to prepare BTRC-T slab specimens (Figure 4). Temporary clamps were used to connect the basalt textile to the decking sheet. The temporary clamps were removed after pouring the concrete. While preparing BTRC-TC same procedure is adopted for another basalt textile (635 mm x 2700 mm) placed in a compression zone of concrete with a clear cover of 20 mm. Since CC composite specimens lack secondary reinforcement, we can study the influence of a basalt textile in a composite slab. Figure 5, Figure 6, and Figure 7 show the position of basalt textiles in respective specimens. Shear span lengths of 250 mm (L/10) and 325 mm (L/7.7) were adopted for the shorter shear span, while 550 mm (L/4.5) and 625 mm (L/4) were used for the longer shear span. The slab specimens were cured using the ponding technique, and the curing duration was 28 days. Using a (14-ton capacity) hydra crane, slabs were moved to the testing set-up once the curing time was over. While lifting the specimen, precautionary measures were taken, and specimens were completely supported throughout transit to the testing facility.

Table 5. Specimen designation.

Specimen ID	Type of concrete	Position of Basalt textile mesh in concrete topping	Length of the shear span (mm)
CC-250	conventional concrete	-	250
CC-625	conventional concrete	-	625
BTRC-T-250	conventional concrete	Tension region	250
BTRC-T-325	conventional concrete	Tension region	325
BTRC-T-550	conventional concrete	Tension region	550
BTRC-T-625	conventional concrete	Tension region	625
BTRC-TC-250	conventional concrete	Tension and compression region	250
BTRC-TC-325	conventional concrete	Tension and compression region	325
BTRC-TC-550	conventional concrete	Tension and compression region	550
BTRC-TC-625	conventional concrete	Tension and compression region	625

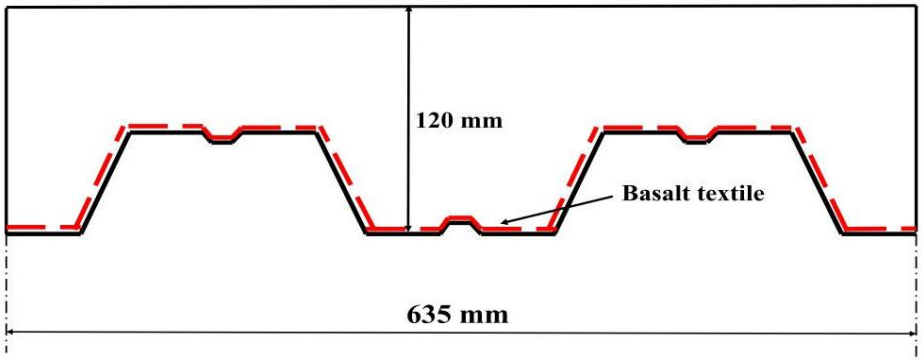

Fig. 5. BTRC-T.

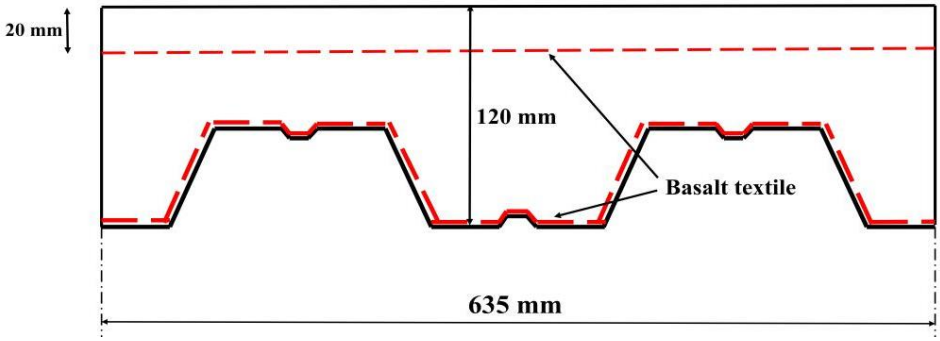

Fig. 6. BTRC-TC.

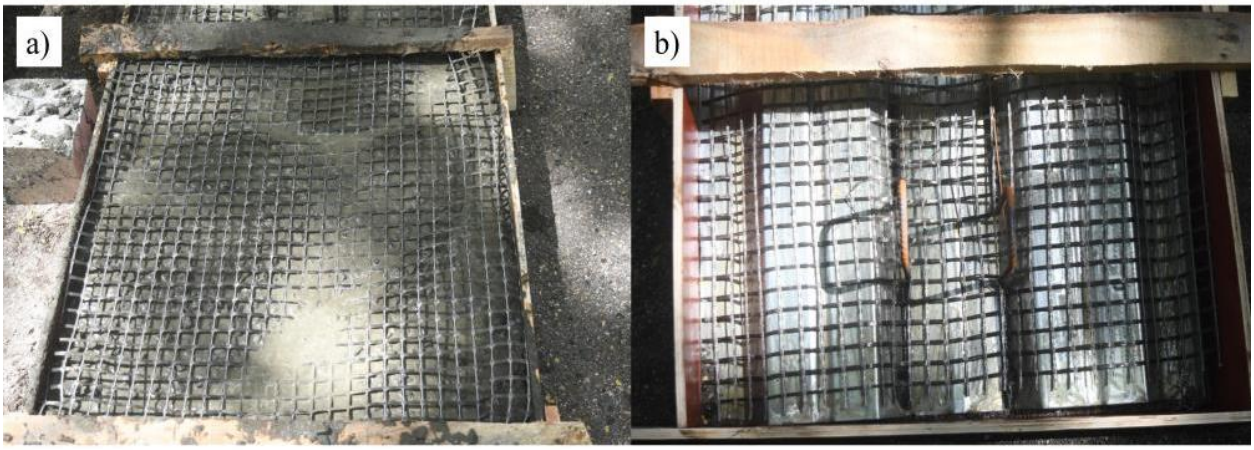

Fig. 7. Position of basalt textile a) Compression region b) Tension region.

3.2. Instrumentation and testing

In this experimental study, A four-point flexural test was carried out on ten full-scale specimens of profiled deck composite slab. The lab tests were carried out in line with Eurocode-4 and BS-5950 [40,41]. Before implementing static loading, Eurocode 4 specifies that the specimen should be subjected to cyclic load to break the chemical interaction between concrete and steel (EN, 2001). Prior to static loading, Eurocode-4 suggested that composite slab specimens be subjected to cyclic loading. The primary objective of cyclic loading is to break the chemical bond between concrete and profiled decking. However, numerous researchers have established that preceding cyclic loading has no effect on the overall load-carrying capacity/shear bond strength of composite flooring [4–6,33] In addition, it has been noted that the initial cracking noise heard during static loading testing is a result of the chemical bond breaking. Therefore, the static loading data obtained after the chemical bond between the slab and the metal deck is completely broken is used to compute the shear bond strength of the composite floor. Conversely, Marimuthu et al. (2007) [4] concluded that the preceding cyclic loading has no significant influence on the slab's load-carrying capacity, and the longitudinal shear bond strength of a composite slab differs negligibly from static loading alone. The test arrangement that is used in this investigation is shown in Figure

8. Specially fabricated roller and hinge support to ensure the simply support condition of the specimens. The test set-up and loading operations were carried out in accordance with the BS5950 and Euro code-4 guidelines [41,42]. All ten composite slab specimens are evaluated under four-point static loading conditions. With the help of the hydraulic jack (20-ton capacity) and spreader beam system, two symmetrical line loads (along the width) were applied to the composite slab specimen at their respective shear span locations. Two linear strain gauges of 60 mm (150 ohms) in length were attached to the surface of the concrete and profiled deck sheet to record their respective strain readings. Utilising five linear variable displacement transducers (LVDTs), the central deflection and relative end slip between profiled decking sheet and concrete topping were determined. A load cell, strain gauges and all five LVDTs were linked to a data collecting system that recorded the results at a rate of 2,000 data samples per second. The midspan deflection was measured using one of the LVDTs, while the remaining four (two LVDTS at each end) were used to determine the relative end slip (in between concrete and the steel sheet). A linear strain gauge (150 ohm) of 60 mm length is utilised to record the maximum strain developed in composite slab. As seen in Figure 8, these strain gauges are installed in the centre of the slab. To record the highest tensile strain created at the profiled decking steel sheet, a strain gauge is mounted at mid-span to the bottom of the profiled deck sheet. One of the strain gauges is attached to the top of the slab specimen in order to measure the maximum compressive strain at the concrete topping's upper fiber. Before installing the strain gauge, the profiled deck sheet and concrete are thoroughly cleaned. The testing was conducted using a displacement control technique, and the load was applied at a rate of 0.01 mm displacement/second till the ultimate failure of the specimen. Shear crack formation and propagation, vertical detachment (between steel and concrete) and the modes of failure were visually observed during testing. The experimental set-up is depicted in Figure 9. Figure 10 shows roller and hinge supports.

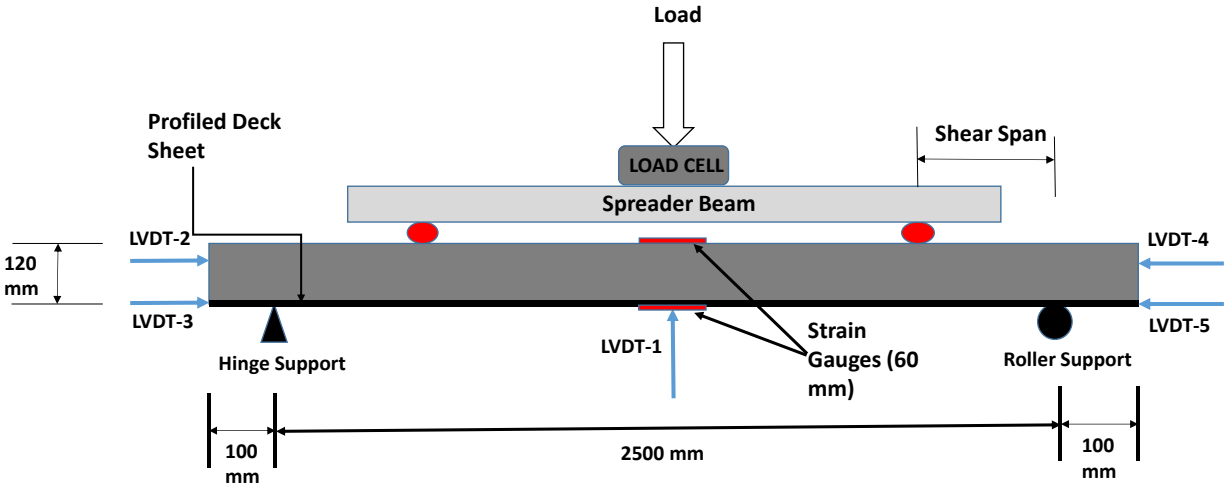

Fig. 8. Schematic view of the experimental set-up.

Fig. 9. Experimental set-up.

Fig. 10. roller support and hinge supports.

4. Results

4.1 General observations

The deflection in the composite slab specimens increased as a result of the increase in the applied static load. It is observed that the specimens with shorter shear spans failed at a higher load than those with longer shear spans. Figures 11, 12, and 13 show how cracks form in BTRC and regular concrete composite slabs.

4.1.1. Longer shear-span specimens

In the first phase of the load-deflection curve for composite slabs with basalt textile (BTRC-T, BTRC-TC), no debonding cracks at the steel-concrete interface were detected. At the same time, visible debonding cracks developed in the composite slab with CC topping (CC). Fine flexural cracks appeared in the middle-third section of the slab (Figs. 11-(a), 12-(a, b), and 13-(a, b)). Compared to a CC composite slab, a composite slab with

basalt textile (BTRC-T, BTRC-TC) exhibits more fine flexural cracks, and these cracks were distributed evenly across the mid-span of the slabs. Additional shear cracks were developed near the loading locations in the second phase. As the imposed load reaches its maximum value, the concrete cracks are extended to the top fiber of the concrete.

4.1.2. shorter shear-span specimens

In the first phase of the loading, horizontal debonding cracks were observed in the composite slab specimens with shorter shear spans. Compared to the specimens with the longer shear span, the shorter shear span specimens failed at a relatively lower deflection. The major shear crack for each specimen was thoroughly formed beneath one of the applied line loads. Specimens with basalt textile (BTRC-T, BTRC-TC) achieved a higher failure load compared to the specimens with CC topping (CC). The interfacial detachment was seen throughout the shear span, causing the applied load to significantly drop while central deflection and end slip continued to increase.

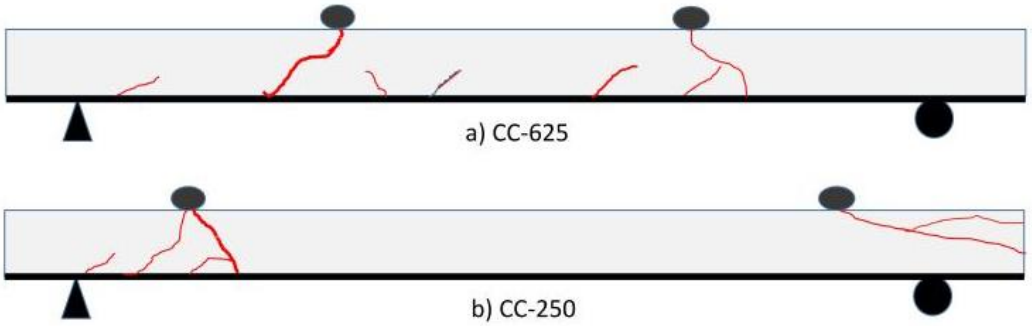

Fig. 11 Crack patterns in CC composite slab specimens.

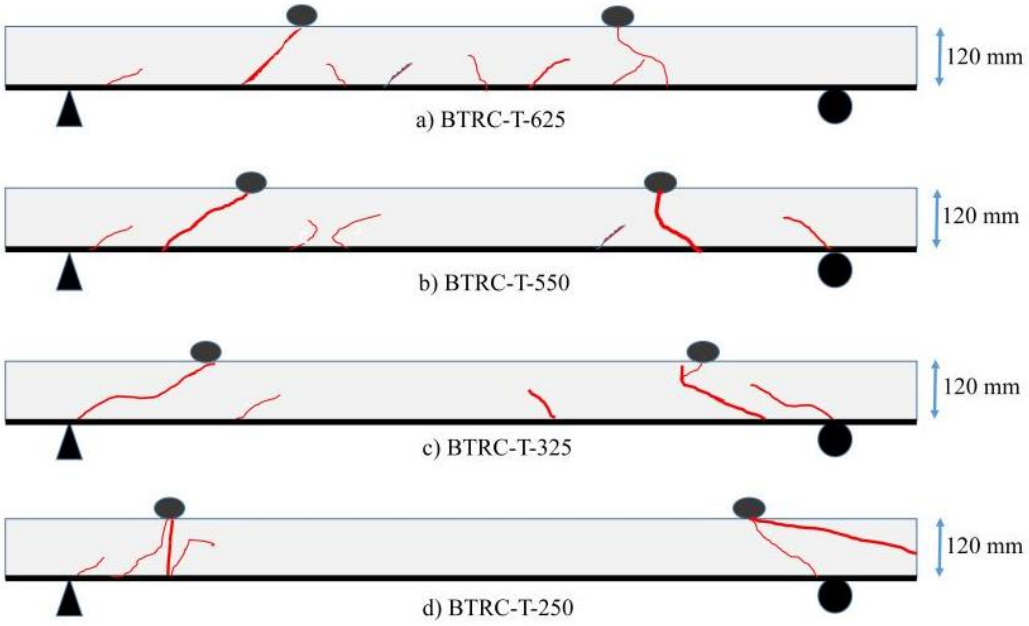

Fig. 12. Crack patterns in BTRC-T composite slab specimens.

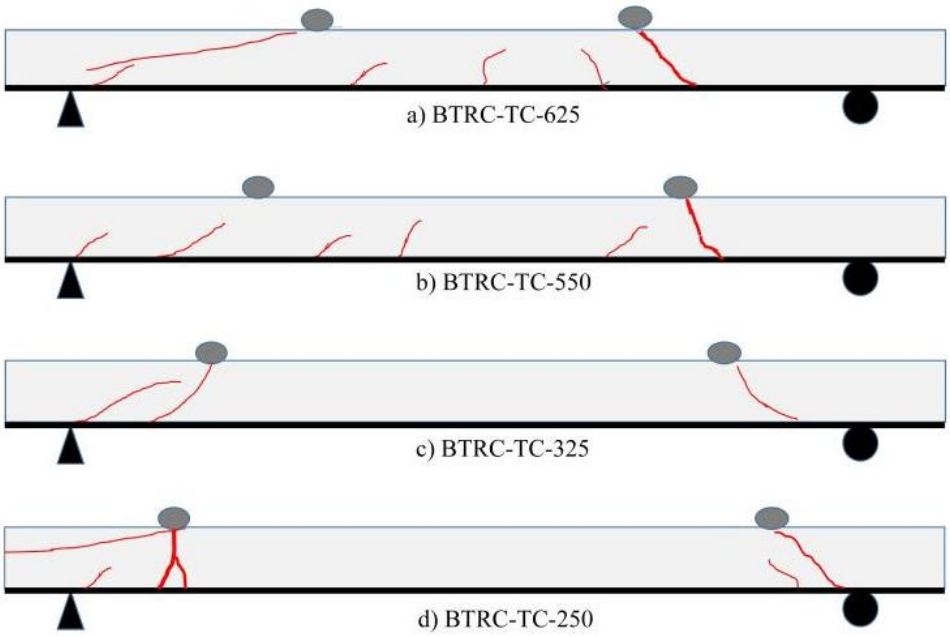

Fig. 13. Crack patterns in BTRC-TC composite slab specimens.

4.2. Load-Deflection response

Figures 14 and 15 depict the relationship between applied load and midspan deflection for shorter and longer shear-span composite slabs, respectively. The failure load of a typical composite slab is considered the load causing a central deflection of L/50 (50 mm) unless failure has already occurred [41]. Figures 16, 17, and 18 show deflected shapes after the ultimate failure of specimens. The ultimate failure load and ultimate deflection of all ten composite slab specimen are shown in Table 6. The typical load-central deflection curve of a composite slab specimen is observed to have three phases. The initial phase is the pre-cracking phase, the second is the debonding phase, and the third is the ultimate failure. During the pre-cracking phase, the load-deflection graph shows a steady slope. In the debonding phase, which follows the pre-cracking phase, the curve becomes non-linear, and bending cracks emerge in the slab. During the debonding phase, shear cracks form, and as one of the shear cracks enlarges, the slab eventually fails, which is known as the ultimate failure of the composite slab. Large deflections in the inelastic zone indicate that composite slabs containing basalt textiles have ductile behaviour (BTRC-T, BTRC-TC). Furthermore, these specimens had significantly higher ductility as compared to the CC composite slab specimens (CC). For the BTRC-TC-250 and BTRC-T-250, the highest measured load at failure was 105.49 kN and 79.47 kN, respectively. With a failure load of 23.38 kN and a corresponding central deflection of 45.62 mm, the CC composite slab with a short shear span had the lowest load-bearing capacity. Specimens containing basalt textile failed at greater loads; this trend is seen in all four types of shear span composite slab specimens. Adding basalt textile to the tension zone of a composite slab significantly increases its strength. The ultimate deflection of specimens with basalt textile (BTRC-TC, BTRC-T) topping is 31%–57% more than that of specimens with CC topping. It is also observed that the

ultimate load-carrying capacity of the composite slab was clearly influenced by the slenderness ratio Ls/dp; specimens with a higher slenderness ratio failed at comparatively lower loads. In specimens with a lower slenderness ratio (L_s/d_p), a sudden drop in applied load at lower deflection was observed. Moreover, the addition of basalt textile in the compression region resisted crack propagation effectively as the ultimate failure load was increased by 20% to 25% over the BTRC-T specimens. The fiber-bridging effect of basalt textile enhanced the composite slab's overall performance.

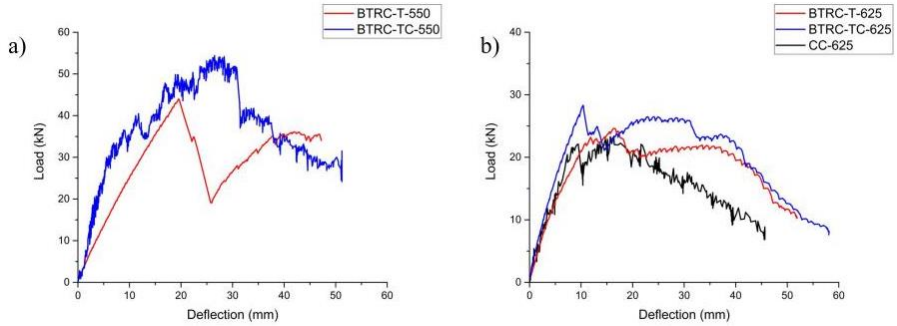

Fig. 14. Load-deflection curves for specimens with longer shear spans a) 550 mm b) 625 mm.

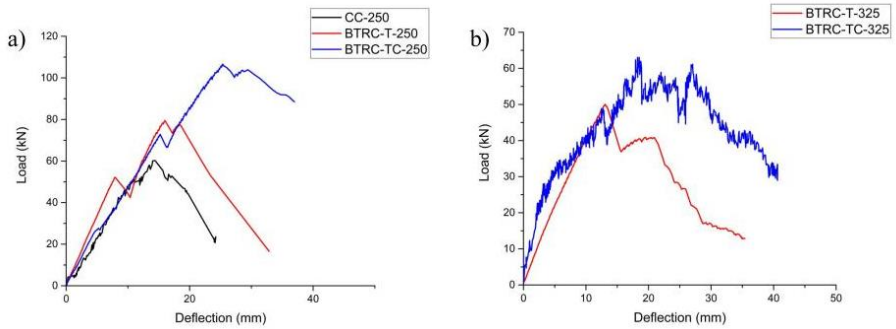

Fig. 15. Load-deflection curves for specimens with shorter shear spans a) 250 mm b) 325 mm.

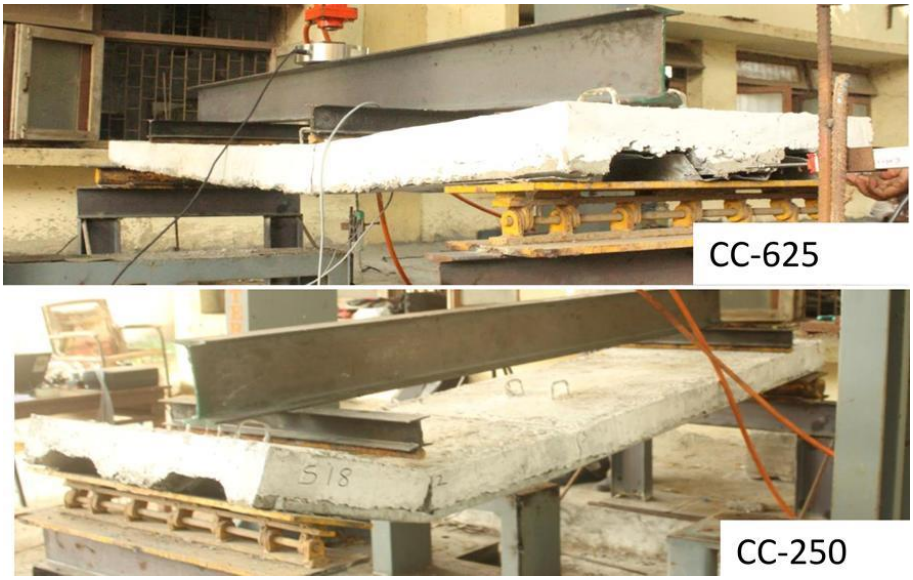

Fig. 16 Deflected shapes of CC composite slab specimens.

Table 6. Load-deflection results.

Specimen id	Load at the first crack (kN)	Ultimate failure load (kN)	Ultimate Deflection (mm)
CC-250	54.54	60.24	24.13
CC-625	12.54	23.38	45.62
BTRC-T-250	68.47	79.47	32.28
BTRC-T-325	35.78	48.77	35.4
BTRC-T-550	29.52	43.56	47.11
BTRC-T-625	15.65	25.38	52.82
BTRC-TC-250	92.58	105.41	36.66
BTRC-TC-325	44.25	61.98	40.61
BTRC-TC-550	38.73	54.05	51.21
BTRC-TC-625	21.45	27.78	58.1

Fig. 17. Deflected shapes of BTRC-TC composite slab specimens.

Fig. 18. Deflected shapes of BTRC-T composite slab specimens.

4.3. Load-Slip response

Two LVDTs at each end were used to detect the differential end slip between the concrete and the profiled decking sheet. As illustrated in Figure 19, one is connected to the concrete surface, while the other is attached to the deck sheet. Eurocode-4 considered longitudinal shear behaviour to be ductile if the failure load exceeds by more than 10% than of load, causing an end slip of 0.1mm (EN, 2001). The ductile failure criteria were met by all ten composite slab specimens. The load slip responses of all ten composite slab specimens according to their shear spans are depicted in Figures 20 and 21.A typical load-end slip plot has three phases: the slip resistance phase, slippage, and ultimate failure. All horizontal shear stresses generated by the applied load are effectively transferred from the concrete to the profiled decking steel sheet during the slip resistance phase. As the load increases, the bond between the decking steel sheet and concrete breaks and slippage is initiated; this phase is termed the slippage phase.as load increases the slippage increases exponentially. **Table 7** represents the load-slip results of all ten

specimens. Typical end slip and vertical separation are depicted in Figure 22. Differential slip has been seen to start at a load of 50% to 60% of the ultimate failure load, which causes a sudden increase in slippage. This slippage is caused by the separation of the concrete and profiled deck sheet at the interface, which can be seen in the noise at the beginning of the load-end slip curves. The interaction between both the concrete and profiled steel deck was weakened at higher loads in the shorter shear span specimens (250 mm and 325 mm); these specimens also exhibited considerably more slippage. An exponential rise in slippage after the loss of shear bond implies an inelastic behaviour of composite slabs with CC topping. Slippage was higher in the CC-250 and CC-625 specimens compared to specimens with basalt textile (BTRC-TC and BTRC-T), attributed to its lower stiffness and modulus of elasticity. The adhesion between the concrete and profiled steel deck was lost at lower loads for the longer shear spans; as a result, lower slippage was recorded for the respective specimens. It was observed that the addition of basalt textile in the tension zone of concrete improved the shear bond significantly. Basalt textile effectively resisted the shear crack propagation, which can be evidenced by the higher slip resisting load. However, the influence of basalt textile in the concrete compression zone on limiting end slippage is relatively ineffectual, but it effectively resisted the vertical separation. The inclusion of basalt textile in a composite slab enhances the structural behaviour of the composite slab as it approaches complete interaction, notably evidenced by lower end slippage.

Table 7. Load-slip results.

Specimen id	Load causing 0.1 mm slip (kN)	End slip (mm)
CC-250	43.03	10.2
CC-625	21.28	5.9
BTRC-T-250	52.34	6.8
BTRC-T-325	44.25	5.2
BTRC-T-550	40.58	4.8
BTRC-T-625	24.58	4.5
BTRC-TC-250	61.52	6.1
BTRC-TC-325	52.34	4.5
BTRC-TC-550	46.86	3.1
BTRC-TC-625	28.02	2.7

Fig. 19 LVDT's arrangements for measuring relative end slip.

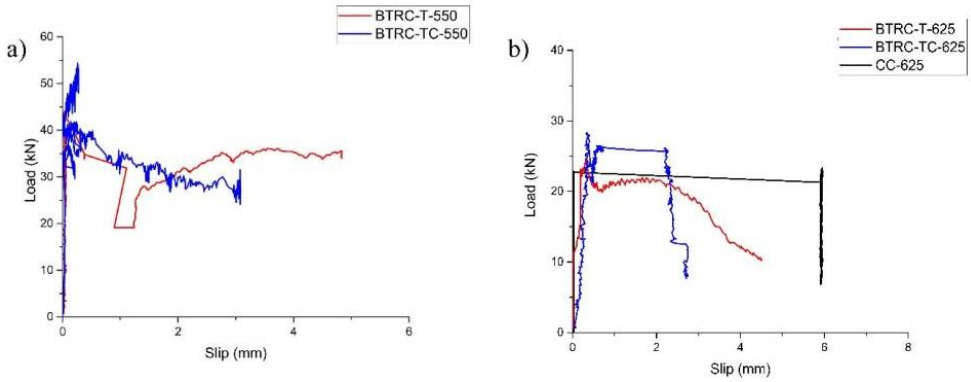

Fig. 20 Load-end slip curves for specimens with longer shear spans a) 550 mm b) 625 mm

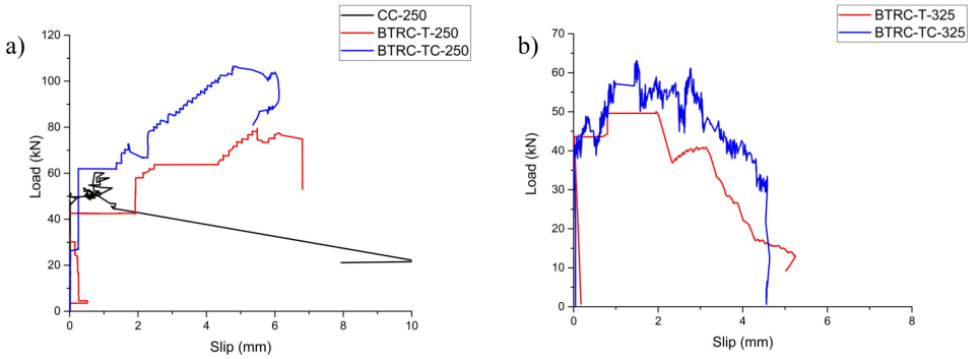

Fig. 21 Load- end slip curves for specimens with shorter shear spans a) 250 mm b) 325 mm

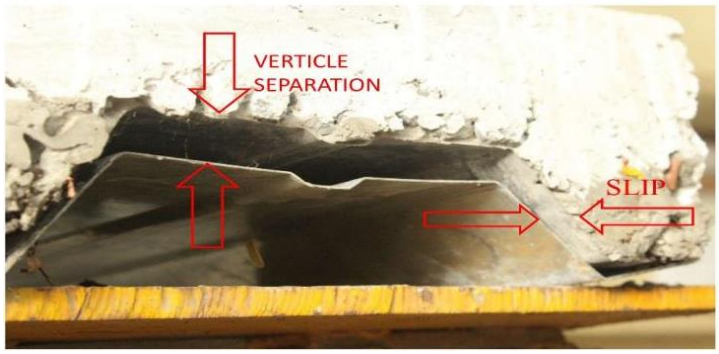

Fig. 22 Typical end slip and vertical separation

4.4 Compressive strain in the concrete surface

A linear strain gauge of 60 mm length (150 ohm) is mounted to the surface of the concrete at the mid-span to record the maximum strain developed in the uppermost fiber of concrete. The highest compressive strain recorded for each composite slab specimen is depicted in Figure 23. Figure 23 demonstrates that the specimen's ultimate compressive strain is proportionate to its ultimate load-carrying capacity. Higher compressive strains indicate better composite performance. It was observed that specimens with a shorter shear span length had higher compressive strains as they had higher load-carrying capacity. Compared to composite slabs with a longer shear span, specimens with a shorter shear span length showed better elastic strain resistance capacity as

they failed at higher loads. None of the composite slab specimens yielded at the concrete's maximum theoretical compressive strain limit of 0.0035. The least compressive strain (112.26 με) is recorded for the CC-250 specimen. It was observed that BTRC-T specimens produced 8.50% to 31.92% more compressive strain than the CC composite slab. Furthermore, basalt textile in the compression region adds 13.45% to 32.46% in compressive strains. Higher compressive strains in a composite slab indicate a specimen with a higher energy-absorbing capacity.

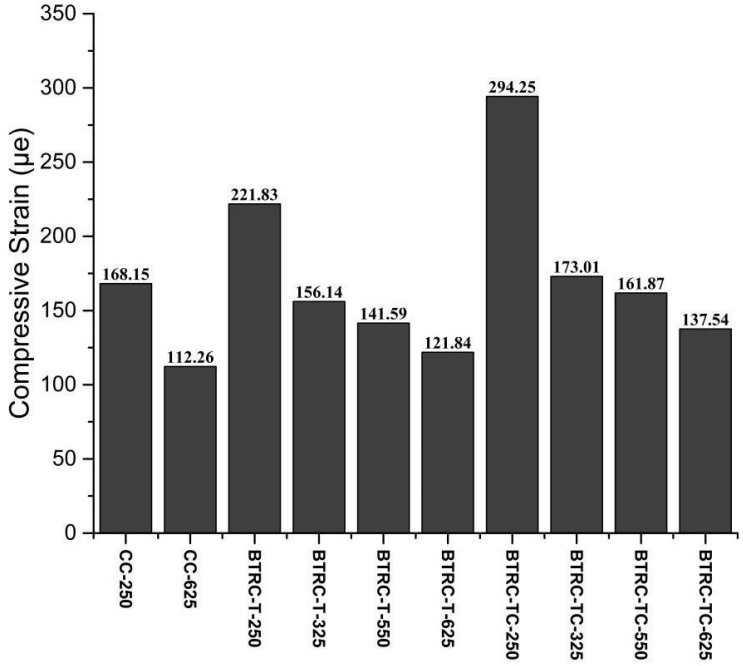

Fig. 23. Compressive strains in concrete topping.

4.5. Tensile strain in profiled deck sheeting

A linear strain gauge of 60 mm in length is installed on the bottom surface of the profiled decking sheet at the centre of the span to record the maximum tensile strain in the decking sheet. The strain readings of the profiled steel sheets are shown in Figure 24. It is observed that tensile strain increases with deflection, but compressive strain increases with load application. In comparison to specimens with a longer shear span, compressive strains are greater for specimens with a shorter shear span. In contrast, specimens with longer shear spans failed at greater deflection, resulting in greater tensile strains than those of specimens with shorter shear spans. Specimens with basalt textile at the tension region yielded greater tensile strain (15.78% to 33.77%) for each shear span length than CC composite slabs. The addition of basalt textile in the compression region increases the tensile strain by 3.56% to 10.03%. It was also observed that none of the composite slab specimens yielded the maximum theoretical tensile strain value of the steel 1619 με ($f$yp/ Es). However, BTRC-T-625 and BTRC-TC-625 specimens failed at 81.77 % to 89.98 % of the maximum theoretical tensile strain capacity of steel, respectively. Evidence of inadequate interaction between the steel sheet and the concrete may be seen in the short-

span slab specimen, where the steel strain is significantly lower than the yield strain. As can be observed in Figure 24, the bottom flange of the steel sheets in the BTRC composite slab specimens received more strain than in the CC slabs for both the shorter and longer shear spans. This behaviour implies that BTRC composite slabs outperformed CC composite slabs in terms of composite action. Higher tensile strains in composite slabs with basalt textiles are attributed to their higher ductility and shear transfer capacity.

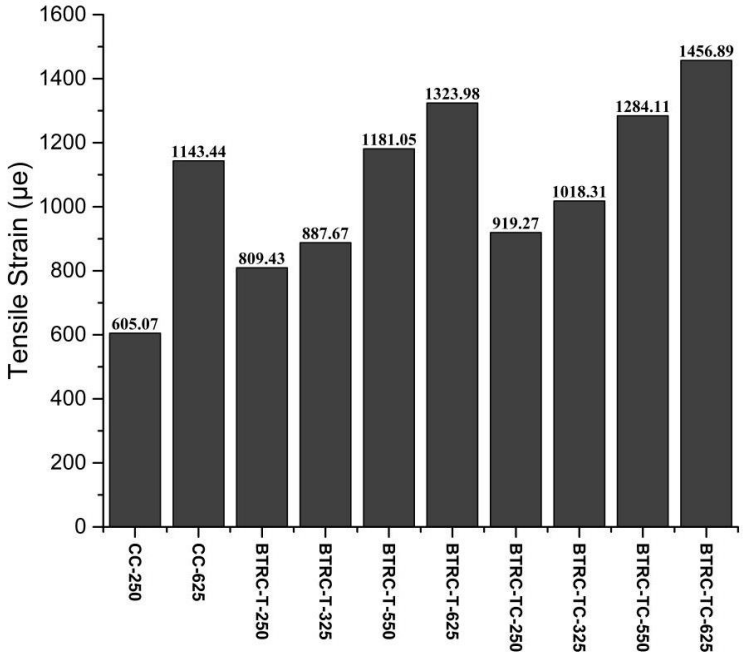

Fig. 24. Tensile strains in the profiled deck sheet.

4.6. Longitudinal shear strength

The degree of connection between concrete and steel elements is crucially vital in composite floor design. Due to the complexity of the analysis of the shear interaction of composite slabs, full-scale flexural tests are essential. The *m-k* (semi-empirical) and partial shear connection (*PSC*) techniques are the two statistical methods given by EC4 for calculating the horizontal shear strength of composite floors [43,44]. These two approaches are utilised in this study to illustrate that BTRC concrete composite slabs have higher longitudinal shear strength than CC-topping composite slabs.

4.6.1 m-k method

The shear transfer capacity of profiled deck composite slab primarily depends upon the *m-k* parameters. These parameters depend upon the slenderness (L_s/d_p) and the frictional coefficient of the composite slab. For composite floors having a horizontal shear bond failure as a mode of failure, Porter and Ekberg Jr (1971) [1] suggested the design equation for the shear bond capacity of composite deck slabs.

$$\sigma_u = \frac{V_t}{bd_p} = m\left(\frac{\rho d_p}{L_s}\right) + k\sqrt{f'} \quad (1)$$

If the compressive strength of concrete varies substantially throughout a set of experiments, equation (1) provides unreliable m and k parameters. Numerous researchers have also

verified that the compressive strength of concrete has no major impact on the shear bond properties of composite slabs [12,43,44]. Equation 2 gives the modified form of the *m-k* method, here to reduce the scattering of the data points concrete strength parameter is omitted, and the ρ is replaced as the ratio of the reinforcement $\left(\frac{A_p}{bd_p}\right)$. This modification is per previous studies, which suggested that the cause of scattering was related to the concrete compressive strength [3]. Later, this technique was accepted by ASCE in the form of the *m-k* method [44].

$$\sigma_{u,rd} = \frac{V_t}{bd_p} = m\left(\frac{A_p}{bL_s}\right) + k \qquad (2)$$

The line equation is represented by equation (2), wherein m is the line's slope, and k signifies the line's vertical intercept. Horizontal shear transmission capacity is calculated using *m-k* parameters; the mechanical interlock between the profiled steel sheet and the concrete is characterised by the m, while the friction coefficient is represented by the k parameter. A graph was drawn for bond strength (V_t / bd_p) against reinforcement ratio (A_p / bL_s) to quantify m and k parameters, and a simple regression analysis was performed. A ten percent reduction line was drawn underneath the original trend line to obtain the m and k values [41]. This decrease was intended to compensate for test variances. Parameters for the m-k plot are listed in Annexure I. For CC and BTRC concrete composite slabs, the m-k curve is drawn (Figure 25-27). from m-k parameters, longitudinal shear strength is calculated using Equation 2 and presented in Table 9. It is observed that with an increase in the length of the shear span, the value of the longitudinal shear strength decreases. The m-k values obtained in this study are compared to those obtained in other studies and presented in Table 10. The BTRC concrete topping has proven to be a preferable alternative to CC topping as it yields maximum horizontal shear strength. It was observed that BTRC-T composite slab achieved 18.37 % more longitudinal shear strength compared to the CC composite slab. Whereas BTRC-TC composite slab improved the longitudinal shear strength by 49.57%. m-k plot for CC concrete composite slabs and BTRC-T concrete composite slabs is shown in Figure 25 and Figure 26, respectively.

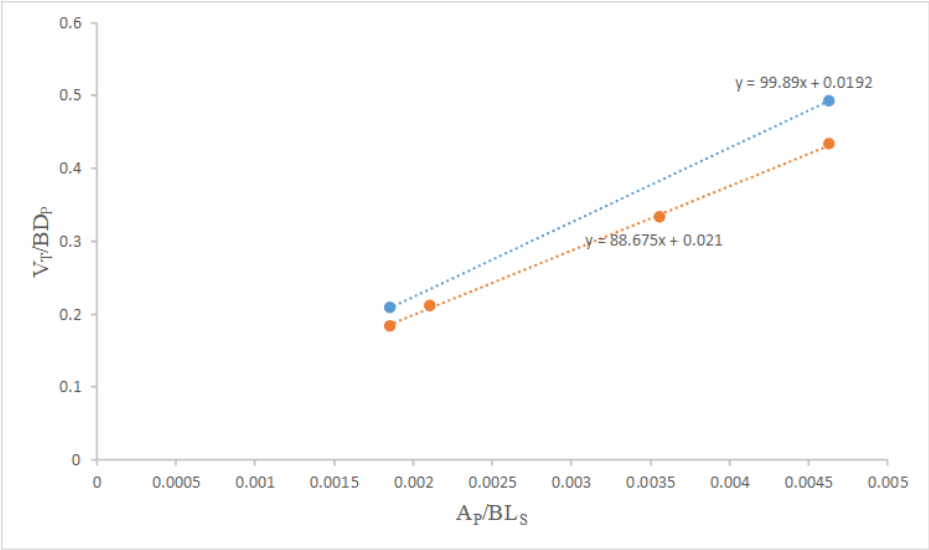

Fig. 25. *m-k* plot for CC concrete composite slabs.

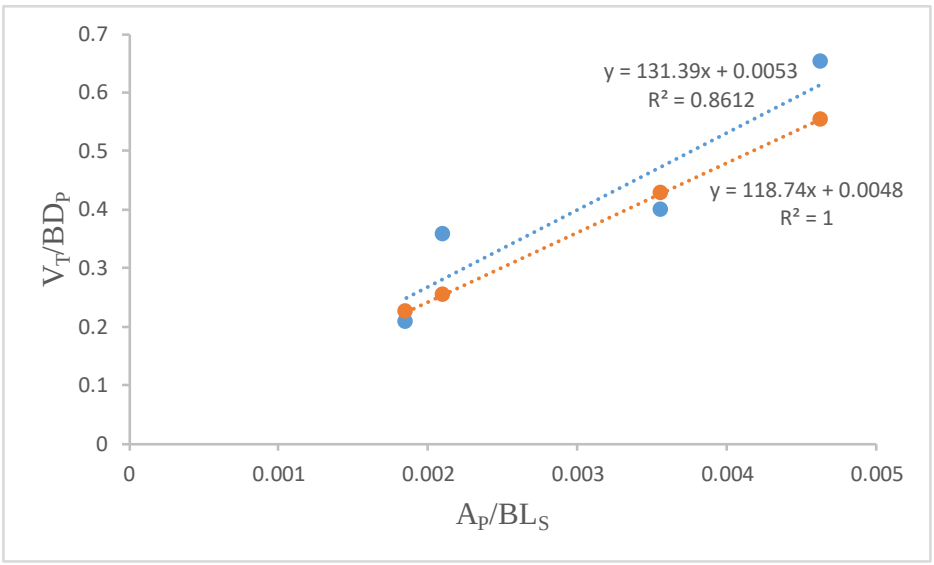

Fig. 26 *m-k* plot for BTRC-T concrete composite slabs.

Table 9. Longitudinal shear strength by the *m-k* method.

Slab ID	*m*	*k*	$\sigma_{u,rd}$ N/mm^2	$\sigma_{u,rd\ avg}$ N/mm^2
BTRC-T-250	118.737	0.00477	0.554	0.364
BTRC-T-325	118.737	0.00477	0.427	
BTRC-T-550	118.737	0.00477	0.254	
BTRC-T-625	118.737	0.00477	0.224	
BTRC-TC-250	169.956	0.05625	0.730	0.458
BTRC-TC-325	169.956	0.05625	0.544	
BTRC-TC-550	169.956	0.05625	0.301	
BTRC-TC-625	169.956	0.05625	0.258	
CC-250	89.901	0.01632	0.432	0.307
CC-625	89.901	0.01632	0.182	

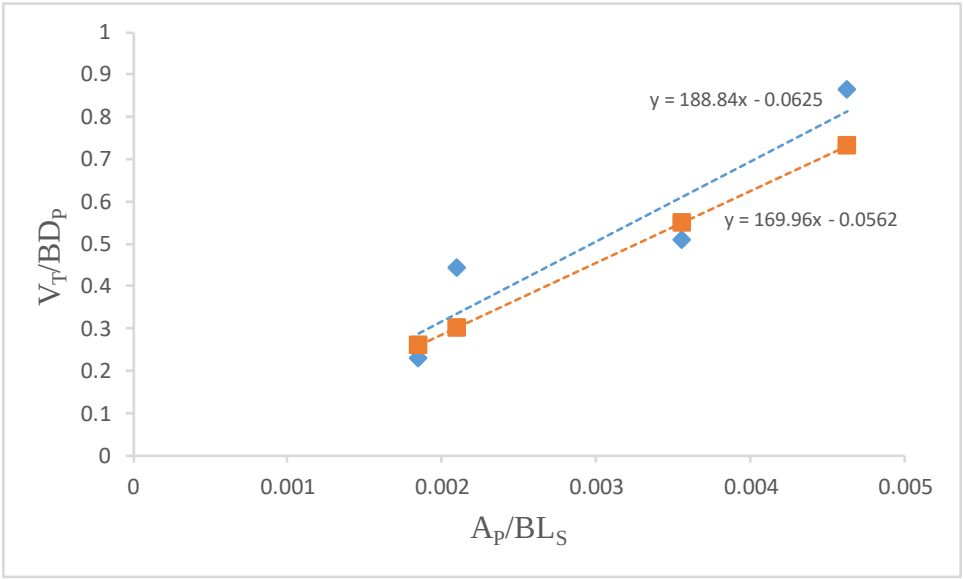

Fig. 27. m-k plot for BTRC-TC concrete composite slabs.

Table 10. *m–k* values compared with those of other authors.

Author	Variable parameters in research	*m* (N/mm^2)	*k* (N/mm^2)
H.D. Wright et al.	Embossment in profiled deck sheet	107.527	0.0401
S. Chen	Chevron Embossements	84.665	0.0221
Marimuthu	Rectangular embossments	87.956	0.0322
K.M.A. Hossain	ECC	345.01	0.0037
	SCC	313.21	0.0395
Bashar S Mohammed	Crumb rubber concrete	80.72	0.037
Xin Li	Fiber-reinforced lightweight aggregate concrete	116.47	0.028
Present Study	BTRC-T	118.73	0.0047
	BTRC-TC	169.95	0.0562

4.6.2. PSC method

The slab is considered to have uniform longitudinal shear stress at the interface of concrete and decking sheet in the PSC approach. A ductile type of failure is required for this method. The PSC approach is used as an alternative to the m-k methodology for calculating the longitudinal shear strength of a composite floor. Johnson (2004) [12] presented an expression for estimating horizontal shear capacity based on the magnitude of shear connection (η) between decking sheet and concrete. The flexural strength of the composite floor was estimated using a rigid plastic model and a fundamental stress block for both the concrete and the profiled steel sheet. The flexural strength was calculated at the two extreme values (null/zero connection and full/complete connection) of the interactions between the concrete and the decking sheet; between these two extremities, the slab has a partial shear connection (Figure 28). In this condition, the compressive force in the concrete Nc is smaller than Ncf and is determined by the intensity of the shear connection, as illustrated in Fig. 29(c) for the slab (with Nc instead of Ncf) and Fig. 29(d) for the sheet.

The depth of the stress block of concrete is,

$$x = \frac{N_c}{b(0.36f_{ck})} \leq h_c$$

In this case,

$Nc = Ncf$

$Ncf = Npa$

$x = hc$

Thus,

$$z = h_t - 0.42x - e_p \frac{(e_p - e)N_C}{N_{cf}}$$

$$M_{pr} = 1.25M_{pa}\left[1 - \frac{N_c}{N_{cf}}\right] \leq M_{pa}$$

$$M_{p,Rd} = N_c z + M_{pr}$$

$$\sigma_{u,} = \frac{\eta N_{cf}}{b(L_S + L_O)} \quad (3)$$

In an attempt to develop an interaction diagram, Annexure II is utilised. From the interaction diagram (Figure 29), the bending moment corresponding to the ultimate load-carrying capacity was used to evaluate the

degree of shear connection (η). The longitudinal shear strength ($\sigma_{u,}$) for each tested composite slab specimen was then calculated using Equation 2, shown in Table 12. Composite slab specimens with only CC-topping reported the lowest longitudinal shear bond strength, however an increment of 7.36 % in longitudinal shear strength (σ_u) is observed for BTRC-T composite slab specimens. Additional basalt textile mesh in the compression region improves the longitudinal shear strength by 136.56 %. Figure 30 shows the PSC curve for NC.

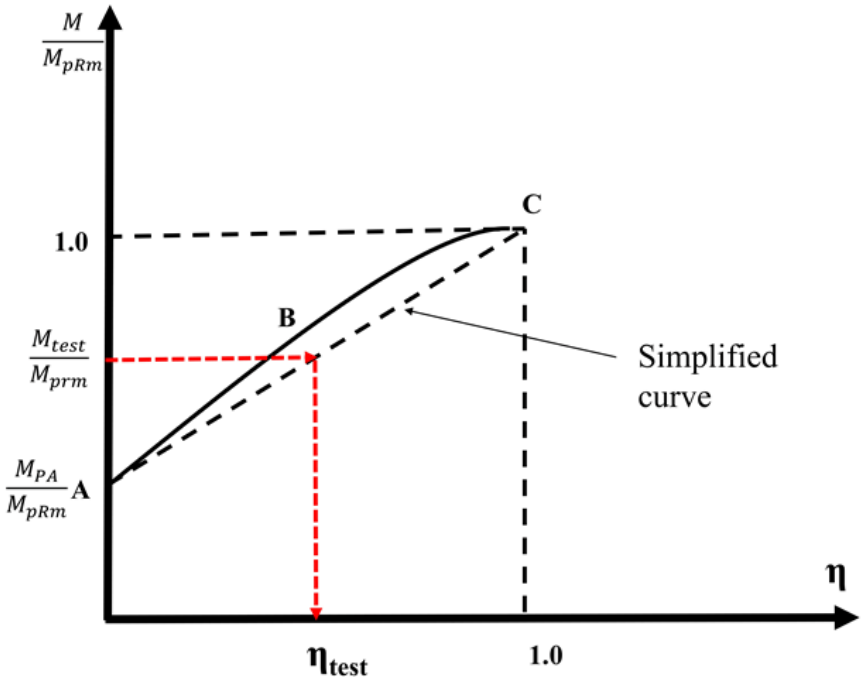

Fig. 28. *PSC* interaction curve.

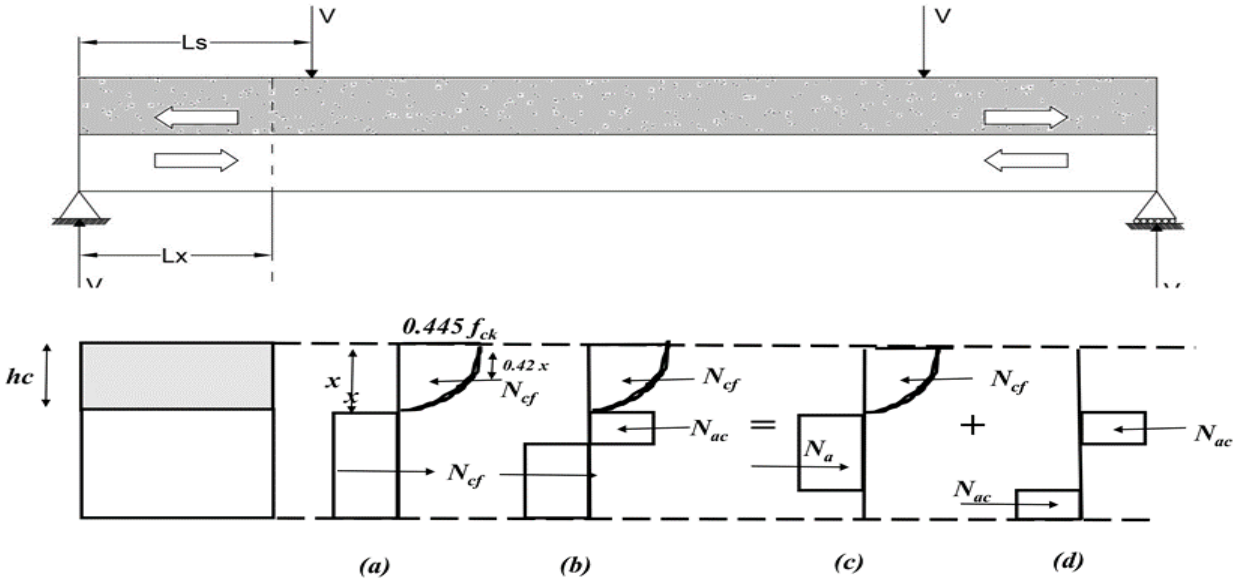

Fig. 29. Partial shear interaction.

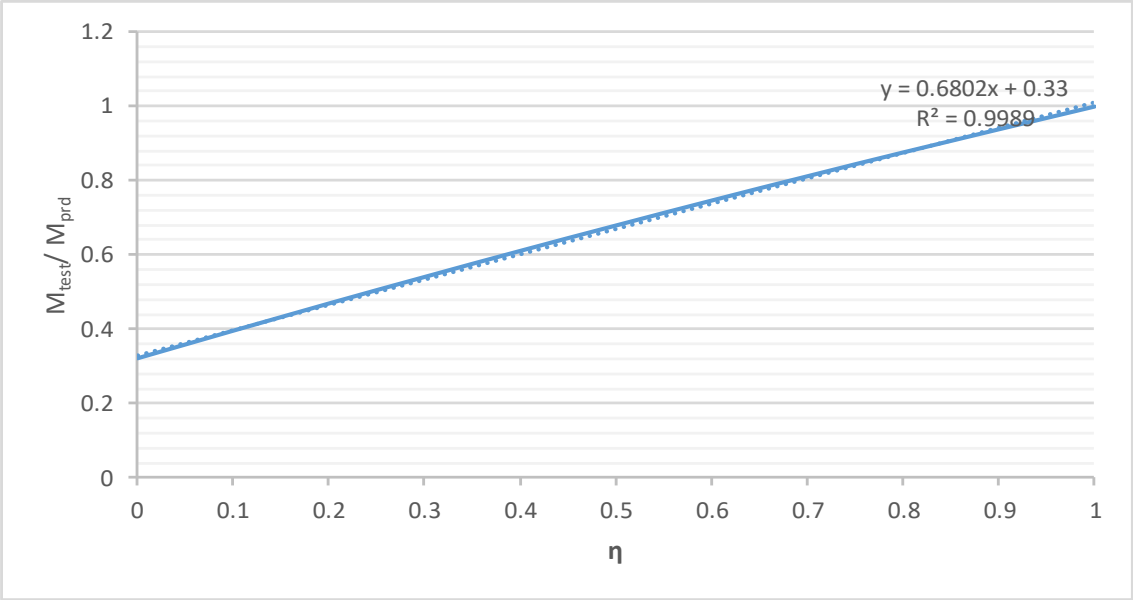

Fig. 30 *PSC* curve for NC.

Table 12. Longitudinal shear strength by PSC method.

Slab ID	M_{test}	M_{test}/M_{prd}	η	$\sigma_{u,rd}$ (Mpa)	$\sigma_{u,rd}$ avg (Mpa)
BTRC-T-250	9.93	0.44	0.15	0.18	0.102
BTRC-T-325	7.93	0.35	0.02	0.03	
BTRC-T-550	11.98	0.53	0.29	0.18	
BTRC-T-625	7.93	0.35	0.02	0.02	
BTRC-TC-250	13.17	0.58	0.36	0.42	0.225
BTRC-TC-325	10.07	0.44	0.16	0.15	
BTRC-TC-550	14.86	0.65	0.47	0.29	
BTRC-TC-625	8.68	0.38	0.07	0.04	
CC-250	30.05	7.51	0.33	0.02	0.095
CC-625	12.72	7.95	0.35	0.17	

Table 13. Average horizontal shear bond strength.

Type of concrete	Average horizontal shear bond strength (N/mm^2)	
	***m-k* method**	**PSC Method**
CC	0.307	0.095
BTRC-T	0.364	0.102
BTRC-TC	0.458	0.225

The longitudinal shear strength of the composite slab is determined using the *m* and *k* values obtained and compared to the PSC technique. Table 13 lists the comparison of values. The longitudinal shear strength calculated by the PSC approach was found to be lower than those obtained by the m–k method, which makes the design more economical. The results in Table 12 shows that adding basalt textile to the tension region of a composite slab enhances the shear bond strength. Basalt textile improves the modulus of elasticity of concrete and also acts as secondary reinforcement. The flexural crack propagation is effectively arrested by the basalt textile in the compression region and prevented the brittle failure.

5. Conclusions

In order to determine longitudinal shear behaviour and failure mechanisms, ten composite slab specimens made of profiled steel sheeting, CC and basalt textile mesh were cast and tested in this work. The specimens were subjected to four-point flexural testing, with a number of key parameters being changed, such as the length of shear span and the use of basalt textile as additional tensile as well secondary reinforcement. The *m-k* technique and the partial shear connection (*PSC*) method specified in European standard EC-4 are used to evaluate the longitudinal shear strength of the composite slabs. The procedures for analysing longitudinal shear bond strength (m-k method, PSC method) are equated and found to be appropriate for this particular type of composite slab.

- Ductile failure observed in all BTRC and CC composite slabs, all composite slab specimens met the EC-4 ductility requirements. Conversely, all failed before reaching their maximum theoretical strain capacity.
- The basalt textile increases the composite slab's rigidity. Therefore, the load-deflection responses are very different from that observed in CC composite slab specimens. The performance of BTRC slabs before and after peak loads is characterised by smooth rising and dropping curves, whereas the performance of CC slabs before and after peak loads is characterised by sudden falls and peaks. This is due to the fact that basalt textiles attempted to prevent crack initiation and propagation during post-crack behaviour, as well as brittle failure of composite slab.
- As the length of the shear span increases, the maximum load-bearing capacity decreases. BTRC-T and BTRC-TC composite slabs outperformed CC composite slabs in load-bearing capacity by 11.03% to 33.33% for equivalent shear span lengths.
- In comparison to CC slabs, BTRC slabs showed reduced end slippage after the loss of chemical bonding, indicating that BTRC performed better in the partial interaction. The BTRC-T composite slab significantly reduces end slippage (from 80.03 % to 178.99 %) compared to a CC composite slab. Results showed that the addition of basalt textile mesh in the compression zone reduced slippage by anywhere from 8.58 % to 32.49 % of BTRC-T

specimens, leading to a better composite action.

- None of the composite slabs attained their theoretical maximum compressive or tensile strain values. The BTRC specimens produced higher strain values than the CC specimens, indicating that the specimens have a greater energy-absorbing capacity, superior composite action, and ductile behaviour. It also shows the specimens' partial shear interaction state. BTRC slabs, on the other hand, attained 81.77 % to 89.98 % interaction without the utilisation of shear connectors. It shows partial shear interaction of the specimens.
- For BTRC composite slabs with steel sheet, the semi-empirical coefficients m and k have values of 169.95 N/mm2 and 0.0562 N/mm2, respectively. Using these parameters, composite slabs made of BTRC-TC with thicker profiled steel sheets can be designed.
- As the shear span length increases, the shear bond strength as evaluated by the m-k method decreases. No similar impact is seen with the PSC approach.
- BTRC composite slabs have a substantially greater longitudinal shear bond strength than CC composite slabs. The BTRC concrete topping has proven to be a preferable alternative to CC topping
- For composite slabs subjected to static load, the m-k methodology yields higher longitudinal shear stress values than the PSC method.

Appendix

A) Horizontal shear bond strength by m-k method

Annexure I. Parameters for the m-k plot

Slab ID	Width of a sheet (mm) B_s	Depth of concrete topping (mm) d_s	Length of shear span (mm) L_s	Area of sheet per meter length (mm) A_P	Vertical shear force (kN) V_e	A_P/B_sL_S	V_e/B_sd_s
BTRC-T-250	635	96	250	735	39.73	0.004629	0.6517
BTRC-T-325			325		24.38	0.003561	0.3999
BTRC-T-550			550		21.78	0.002104	0.3572
BTRC-T-625			625		12.6	0.001852	0.2081
BTRC-TC-250			250		52.70	0.004629	0.8644
BTRC-TC-325			325		30.99	0.003561	0.5083
BTRC-TC-550			550		27.02	0.002104	0.4432
BTRC-TC-625			625		13.89	0.001852	0.2278
CC-250			250		30.05	0.004743	0.492
CC-625			625		12.72	0.001897	0.208

b) Horizontal shear bond strength by PSC method

Annexure II. PSC method calculations for CC.

$\eta = \frac{Nc}{Ncf}$	$N_c = \eta * N_{cf}$ (kN)	$M_{pr} = 1.25$ Mpa $(1 - \frac{Nc}{Ncf})$ (kNm)	$Z = ht - 0.5\eta x_{pl} - e$ (mm)	$M_{rm} = Nc*z + M_{pr}$ (kNm)	M_{test}/M_{prd}
0	0	7.25	95.21	7.25	0.3225
0.2	51.204	5.8	93.872	10.60	0.4718
0.4	102.408	4.35	92.534	13.82	0.6150
0.6	153.612	2.9	91.196	16.90	0.7522
0.8	204.816	1.45	89.858	19.85	0.8832
1	256.02	0	88.52	22.66	1.0000

Where M_{pa} = **5.8** kNm/m , e = **24.79 mm** (data from manufacturer of profiled deck sheet)

$N_{cf} = A_p * f_{yp}$ = 753*340 = **256.02** kN/m,

h_t = 120-24.79= **95.21** mm

$x_{pl} = N_{cf}/(b*0.85_{fck})$ = 256020/(635*0.85***35.32**) =**13.42** mm,

$M_{p,Rd} = N_{cf}\ (d_p - 0.5x)$ = 256020 *(95.21 - 0.5***13.38**) = **22.66** kNm/m.

Declaration of competing interest

The authors declare that they have no known competing financial interests or personal relationships that could have appeared to influence the work reported in this paper.

Conflict of interest

The authors disclose no conflict of interest.

References

[1] Porter ML, Ekberg Jr CE. Investigation of cold-formed steel-deck-reinforced concrete floor slabs 1971.

[2] Daniels BJ, Crisinel M. Composite slab behavior and strength analysis. Part II: Comparisons with test results and parametric analysis. J Struct Eng 1993;119:36–49.

[3] Johnson RP, Shepherd AJ. Resistance to longitudinal shear of composite slabs with longitudinal reinforcement. J Constr Steel Res 2013;82:190–4. https://doi.org/10.1016/j.jcsr.2012.12.005.

[4] Marimuthu V, Seetharaman S, Arul Jayachandran S, Chellappan A, Bandyopadhyay TK, Dutta D. Experimental studies on composite deck slabs to determine the shear-bond characteristic values of the embossed profiled sheet. J Constr Steel Res 2007;63:791–803. https://doi.org/10.1016/j.jcsr.2006.07.009.

[5] Hedaoo N, Gupta L, Ronghe G. Design of composite slabs with profiled steel decking: a comparison between experimental and analytical studies. Int J Adv Struct Eng 2012;4:1. https://doi.org/10.1186/2008-6695-3-1.

[6] Gholamhoseini A, Gilbert RI, Bradford MA, Chang ZT. Longitudinal shear stress and bond–slip relationships in composite concrete slabs. Eng Struct 2014;69:37–48. https://doi.org/10.1016/j.engstruct.2014.03.008.

[7] Calixto J, Lavall AC, Melo CB, Pimenta RJ, Monteiro RC. Behaviour and strength of composite slabs with ribbed decking. J Constr Steel Res 1998;46:211–2. https://doi.org/10.1016/S0143-974X(98)00127-8.

[8] Ollgaard JG, Slutter RG, Fisher JW. Shear strength of stud connectors in lightweight and normal-weight concrete. Eng J 1971;8:55–64.

[9] Porter ML, Greimann LF. Shear-bond strength of studded steel deck slabs 1984.

[10] Mäkeläinen P, Sun Y. The longitudinal shear behaviour of a new steel sheeting profile for composite floor slabs. J Constr Steel Res 1999;49:117–28. https://doi.org/10.1016/S0143-974X(98)00211-9.

[11] Chen S. Load carrying capacity of composite slabs with various end constraints. J Constr Steel Res 2003;59:385–403. https://doi.org/10.1016/S0143-974X(02)00034-2.

[12] Johnson RP. Composite Structures of Steel and Concrete. Wiley; 2004. https://doi.org/10.1002/9780470774625.

[13] Lauwens K, Douchy J, Fortan M, Arrayago I, Mirambell E, Van Gysel A, et al. 08.10: Experimental study of ferritic stainless steel composite slabs. Ce/Papers 2017;1:1909–18. https://doi.org/10.1002/cepa.235.

[14] Abdullah R, Samuel Easterling W. New evaluation and modeling procedure for horizontal shear bond in composite slabs. J Constr Steel Res 2009;65:891–9. https://doi.org/10.1016/j.jcsr.2008.10.009.

[15] Siddh SP, Patil YD, Patil HS. Experimental studies on behaviour of composite slab with profiled steel sheeting. Mater Today Proc 2017;4:9792–6. https://doi.org/10.1016/j.matpr.2017.06.268.

[16] Daniels BJ, O'Leary D, Crisinel M. The analysis of composite slabs with profiled sheeting using a computer based semi-empirical partial interaction approach 1990.

[17] Fallah MM, Sharbatdar M, Kheyroddin A. Experimental strengthening of the two-way reinforced concrete slabs with high performance fiber reinforced cement composites (HPFRCC) prefabricated sheets. J Rehabil Civ Eng 2019;7:1–17.

[18] Lakshmikandhan KN, Sivakumar P, Ravichandran R, Jayachandran SA. Investigations on Efficiently Interfaced Steel Concrete Composite Deck Slabs. J Struct 2013;2013:1–10. https://doi.org/10.1155/2013/628759.

[19] Mäkeläinen P, Sun Y. Development of a new profiled steel sheeting for composite slabs. J Constr Steel Res 1998;46:220. https://doi.org/10.1016/S0143-974X(98)80021-7.

[20] Lopes E, Simoes R. Experimental and analytical behaviour of composite slabs. Steel Compos Struct An Int J 2008;8:361–88.

[21] Brückner A, Ortlepp R, Curbach M. Textile reinforced concrete for strengthening in bending and shear. Mater Struct 2006;39:741–8. https://doi.org/10.1617/s11527-005-9027-2.

[22] Hegger J, Voss S. Investigations on the bearing behaviour and application potential of textile reinforced concrete. Eng Struct 2008;30:2050–6. https://doi.org/10.1016/j.engstruct.2008.01.006.

[23] Donnini J, Corinaldesi V, Nanni A. Mechanical properties of FRCM using carbon fabrics with different coating treatments. Compos Part B Eng 2016;88:220–8. https://doi.org/10.1016/j.compositesb.2015.11.012.

[24] Xu S, Krüger M, Reinhardt H-W, Ožbolt J. Bond Characteristics of Carbon, Alkali Resistant Glass, and Aramid Textiles in Mortar. J Mater Civ Eng 2004;16:356–64.

https://doi.org/10.1061/(ASCE)0899-1561(2004)16:4(356).

[25] Rathod N, Gonbare M, Pujari M. Basalt Fiber Reinforced Concrete. Int J Sci Res 2013:359–61.

[26] Sim J, Park C, Moon DY. Characteristics of basalt fiber as a strengthening material for concrete structures. Compos Part B Eng 2005;36:504–12. https://doi.org/10.1016/j.compositesb.2005.02.002.

[27] High C, Seliem HM, El-Safty A, Rizkalla SH. Use of basalt fibers for concrete structures. Constr Build Mater 2015;96:37–46. https://doi.org/10.1016/j.conbuildmat.2015.07.138.

[28] Jiang CH, McCarthy TJ, Chen D, Dong QQ. Influence of Basalt Fiber on Performance of Cement Mortar. Key Eng Mater 2010;426–427:93–6. https://doi.org/10.4028/www.scientific.net/KEM.426-427.93.

[29] Alnahhal W, Aljidda O. Flexural behavior of basalt fiber reinforced concrete beams with recycled concrete coarse aggregates. Constr Build Mater 2018;169:165–78. https://doi.org/10.1016/j.conbuildmat.2018.02.135.

[30] Larrinaga P, Chastre C, Biscaia HC, San-José JT. Experimental and numerical modeling of basalt textile reinforced mortar behavior under uniaxial tensile stress. Mater Des 2014;55:66–74. https://doi.org/10.1016/j.matdes.2013.09.050.

[31] Liu S, Wang X, Rawat P, Chen Z, Shi C, Zhu D. Experimental study and analytical modeling on tensile performance of basalt textile reinforced concrete. Constr Build Mater 2021;267:120972. https://doi.org/10.1016/j.conbuildmat.2020.120972.

[32] Du Y, Zhang M, Zhou F, Zhu D. Experimental study on basalt textile reinforced concrete under uniaxial tensile loading. Constr Build Mater 2017;138:88–100. https://doi.org/10.1016/j.conbuildmat.2017.01.083.

[33] Waldmann D, May A, Thapa VB. Influence of the sheet profile design on the composite action of slabs made of lightweight woodchip concrete. Constr Build Mater 2017;148:887–99. https://doi.org/10.1016/j.conbuildmat.2017.04.193.

[34] Hossain KMA, Alam S, Anwar MS, Julkarnine KMY. High performance composite slabs with profiled steel deck and Engineered Cementitious Composite – Strength and shear bond characteristics. Constr Build Mater 2016;125:227–40. https://doi.org/10.1016/j.conbuildmat.2016.08.021.

[35] Luttrell LD, Davison JH. Composite slabs with steel deck panels 1973.

[36] IS 8112: Specification for 43 grade ordinary Portland cement 2013.

[37] IS 10262 : Concrete Mix Proportioning — Guidelines 2009.

[38] IS 516: Method of Tests for Strength of Concrete 2014.

[39] IS 456: Plain and Reinforced Concrete - Code of Practice 2000.

[40] Test methods for tensile properties of carbon fiber multifilament 2005.

[41] Johnson RP, Anderson D. EN1994 Eurocode 4: Design of composite steel and concrete structures. Civ Eng 2001;144:33–8. https://doi.org/10.1680/cien.144.6.33.40615.

[42] Standard B. 5950" Structural use of steelwork in building" Part 1. Br Stand Inst 1985.

[43] de Andrade SAL, Vellasco PCG d. S, da Silva JGS, Takey TH. Standardized composite slab systems for building constructions. J Constr Steel Res 2004;60:493–524. https://doi.org/10.1016/S0143-974X(03)00126-3.

[44] Engineers ASC. Standard for the Structural Design of Composite Slabs and Standard Practice for Construction and Inspection of Composite Slabs: ANSI/ASCE 3-91, ANSI Approved December 11, 1992 ; Standard Practice for Construction and Inspection of Composite Slabs : ANSI/ASCE 9-91, ANSI Approved December 11, 1992. American Society of Civil Engineers; 1994.